ISSN 0021-3640, JETP Letters, 2008, Vol. 88, No. 11, pp. 747–751. © Pleiades Publishing, Ltd., 2008.

Proximity-Induced Superconductivity in Graphene¶

M. V. Feigel'man, M. A. Skvortsov, and K. S. Tikhonov

Landau Institute for Theoretical Physics, Russian Academy of Sciences, Moscow, 119331 Russia
Moscow Institute of Physics and Technology, Moscow, 141700 Russia
e-mail: feigel@landau.ac.ru

Received October 27, 2008

We propose a way of making graphene superconductive by putting on it small superconductive islands which cover a tiny fraction of graphene area. We show that the critical temperature, T_c, can reach several Kelvins at the experimentally accessible range of parameters. At low temperatures, $T \ll T_c$, and zero magnetic field, the density of states is characterized by a small gap $E_g \le T_c$ resulting from the collective proximity effect. Transverse magnetic field $H_g(T) \propto E_g$ is expected to destroy the spectral gap driving graphene layer to a kind of a superconductive glass state. Melting of the glass state into a metal occurs at a higher field $H_{g2}(T)$.

PACS numbers: 74.20.-z, 74.78.-w, 74.81.-g

DOI: 10.1134/S0021364008230100

Among numerous fascinating properties, graphene [1, 2] provides a unique possibility to study the phenomenon of proximity-induced superconductivity in very favorable conditions. Experimental studies of the Josephson current through graphene in standard wide planar SNS junctions [3] have shown that proximity effect in graphene is qualitatively similar to the one known for usual dirty metals. In this Letter, we show that even a tiny amount of graphene area covered by small superconductive islands (with good electric contact to graphene) can lead to a macroscopically superconductive state of the graphene film, with T_c in the Kelvin range.

We consider a system of superconductive (SC) islands of radius a (with the typical value of a few tens of a nanometer) placed approximately uniformly on top of a graphene layer (with the typical distance between the islands b in the sub-micron range) shown in Fig. 1. We assume that b is much larger than both a and the graphene mean free path l. Moreover, present theory will be limited by the case $l \lesssim a$ when electron motion in graphene is diffusive at all relevant scales. We will not be particulary interested in phenomena in the vicinity of the graphene neutral point, assuming relatively large gate potentials $|V_g| \ge 10$ V, and carrier density $n \ge 10^{12}$ cm^2. We assume graphene Fermi energy $E_F \gg \Delta_0 \gg T_c$, where Δ_0 is the island's superconductive gap. Graphene sheet can be either single- or few-layered: the only relevant features are (i) high diffusion constant $D \ge 10^2$ cm^2/s, and (ii) very low (in comparison with metals) electron density, which allows to combine moderate values of dimensionless conductance $g = (\hbar/e^2R_\square) \ge 3$ with high Thouless energy $E_{\rm Th} = \hbar D/b^2$. Not very large values of sheet conductance g are practically favorable to avoid suppression of superconductivity in small SC islands due to the inverse proximity effect (the latter can be neglected provided that $G_{\rm tot}\delta \le \Delta_0$, where $G_{\rm tot}^{-1} = G_{\rm int}^{-1} + \ln(b/a)/2\pi g \ll 1$ is the total normal-state resistance from the island to the graphene sheet, $G_{\rm int}$ is the SC-graphene interface conductance, and δ is level spacing in the island).

Below we treat graphene as a normal diffusive 2D metal within the standard approach based on the Usadel equation [4]; its applicability to diffusive graphene was proven in Ref. [5, 6]. The intrinsic Cooper channel interaction in graphene can be neglected due to its low DOS [7]. Similarly, phonon-induced attraction is also weak.

Proximity-coupling and transition temperature. We start with calculating the Josephson coupling energy between two superconductive islands of radius a separated by distance $b \gg a$, neglecting the presence of other islands. Such a pair-wise approximation is adequate for determination of T_c, but breaks down at $T \le$

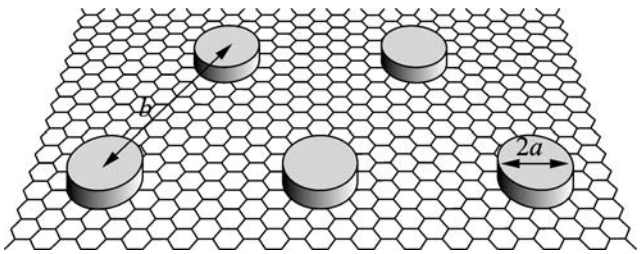

Fig. 1. Graphene film covered by superconducting islands.

¶The article is published in the original.

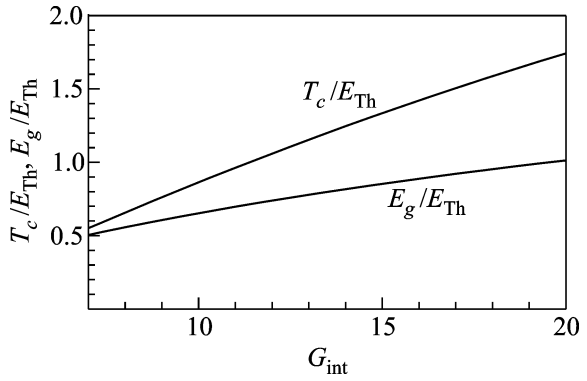

Fig. 2. The critical temperature, T_c, and the zero-temperature spectral gap, E_g, vs. the interface conductance $G_{\rm int}$ (the sheet conductance $g = 6$, and $b/a = 10$).

$T_c/\ln(b/a)$, as shown below. For the single SC island on graphene, the Matsubara-space Usadel equation for the spectral angle θ_ω and corresponding boundary conditions [8] read, as

$$D\nabla^2\theta_\omega - 2|\omega|\sin\theta_\omega = 0, \quad (1)$$

$$\left[g\frac{\partial\theta_\omega}{\partial r} + \frac{G_{\rm int}}{2\pi a}\cos\theta_\omega\right]\Bigg|_{r=a} = 0. \quad (2)$$

The normal (G_ω) and anomalous (F_ω) components of the matrix Green function in the Nambu–Gorkov space are expressed via the spectral angle θ_ω and the order parameter phase φ as $G_\omega(\mathbf{r}) = \cos\theta_\omega(\mathbf{r})$ and $F_\omega(\mathbf{r}) = e^{i\varphi}\sin\theta_\omega(\mathbf{r})$. The full matrix structure of the anomalous Green function $\check{F}_\omega$ with the valley and spin spaces included (Pauli matrices $\hat{\pi}$ and $\hat{s}$, respectively) is determined by the usual s-wave pairing in the SC islands: $\check{F}_\omega \propto \hat{\pi}_x\hat{s}_y$. The interface conductance $G_{\rm int}$ is treated below as a phenomenological parameter which accounts for the Fermi velocity mismatch and a potential barrier on the graphene-metal interface [9].

It is crucial for further analysis that the two-island generalization of the nonlinear problem (1), (2) can be linearized while calculating the Josephson current at inter-island distances $b \gg a$. Indeed, the total current can be calculated by integrating the current density over the middle line between the islands, on the distance $\rho_{1,2} \geq b/2$ from them. This procedure also involves summation over Matsubara energies $\omega_n = \pi T(2n+1)$, with the major contribution to the sum coming from $\omega_n \sim E_{\rm Th}$. At such ω_n and $\rho_{1,2}$ the spectral angle θ is small, and linearization of Eqs. (1) and (2) leads to the solution

$$\theta_\omega(r) = A(\omega)K_0\left(\frac{r}{L_\omega}\right), \quad A(\omega) = \frac{\Theta(t_\omega)}{\ln(L_\omega/a)}, \quad (3)$$

with $L_\omega = \sqrt{D/2\omega}$, $t_\omega = (G_{\rm int}/2\pi g)\ln(L_\omega/a)$, and $\Theta(t)$ solving the equation $\Theta(t) = t\cos\Theta(t)$. The function $A(\omega)$ evolves between the tunnel and diffusive limits as

$$A(\omega) = \begin{cases} G_{\rm int}/(2\pi g), & G_{\rm int} \ll 2\pi g/\ln(L_\omega/d), \\ \pi/[2\ln(L_\omega/d)], & G_{\rm int} \gg 2\pi g/\ln(L_\omega/d), \end{cases} \quad (4)$$

and is always small for $\ln(L_\omega/a) \gg 1$. Thus the Josephson current $I(\varphi) = I_c\sin\varphi$ between two SC islands with different phases, $\varphi_1 - \varphi_2 = \varphi$, can be calculated using the linearized two-island solution for the anomalous Green function: $F_\omega(\mathbf{r}) = e^{i\varphi_1}\sin\theta_\omega(|\mathbf{r} - \mathbf{r}_1|) + e^{i\varphi_2}\sin\theta_\omega(|\mathbf{r} - \mathbf{r}_2|)$. The standard calculation of the Josephson energy $E_J = (\hbar/2e)I_c$ then leads to

$$E_J(b, T) = 4\pi gT\sum_{\omega_n > 0} A^2(\omega_n)P(\sqrt{\omega_n/8E_{\rm Th}}), \quad (5)$$

where $P(z) = z\int_0^\infty K_0(z\cosh t)K_1(z\cosh t)dt$.

A two-dimensional array of SC islands with the coupling energies (5) undergoes the Berezinsky–Kosterlitz–Thouless transition at

$$T_c = \gamma E_J(b, T_c), \quad (6)$$

where the numerical coefficient γ depends on the array structure. Below we will assume that the SC islands form a triangular lattice, in which case $\gamma \approx 1.47$ [10]. For the interface conductance $G_{\rm int}$ comparable with the sheet conductance g, one finds the transition temperature $T_c \sim E_{\rm Th}$. In general, T_c can be obtained by numerical solution of Eq. (6) using Eqs. (3) and (5). The result obtained for the ratio $T_c/E_{\rm Th}$ as a function of $G_{\rm int}$ for $g = 6$ ($R_\square \approx 700\ \Omega$) and $b/a = 10$ is presented in Fig. 2. With the graphene diffusion constant $D = 500$ cm^2/s (see, e.g., [11]) and $b = 0.5$ μm, one estimates $E_{\rm Th} \approx 1.5$ K, leading to T_c in the range 1–3 K for $5 < G_{\rm int} < 20$.

Low temperatures: spectral gap and order parameter. Now we switch to the low-temperature range $T \ll T_c$ and consider the issue of the spectral gap for the excitation above the fully coherent ground state (with all phases φ_i equal). The density of states $\nu(E) = \nu_0{\rm Re}\cos\theta(E)$ is determined then by the periodic solution of Eqs. (1) and (2), analytically continued to real energies: $|\omega| \longrightarrow iE$. This periodic problem is equivalent to the one defined within the single (hexagonal) elementary cell, supplemented by the additional condition $\mathbf{n}\nabla\theta|_{\mathbf{r}\in\Gamma} = 0$, where Γ is the cell boundary. Solution of the Usadel equations for such a geometry leads to formation of the spectral gap E_g similar to the minigap for one-dimensional SNS junctions [12]. To find it, we write $\theta(\mathbf{r}) = \pi/2 + i\psi(\mathbf{r})$ and determine the spectral boundary as the value of E where equation

$$D\nabla^2\psi + 2E\cosh\psi = 0 \quad (7)$$

ceases to have solutions with real $\psi(\mathbf{r})$ [13]. At large $\ln(b/a)$ one may approximate the hexagonal boundary Γ of the elementary cell by the circle of radius $R = b/2$. For the ideally transparent interface, solution of the radially symmetric Eq. (7) gives for the value of the zero-temperature spectral gap:

$$E_g \approx \frac{\hbar D/R^2}{1.5\ln(R/a) - 1.2} \approx \frac{2.65E_{\rm Th}}{\ln(b/4a)}. \quad (8)$$

Decreasing the interface conductance $G_{\rm int}$ leads to the suppression of the minigap, as shown in Fig. 2.

In the limit of large $\ln(b/a)$, the spectral gap $E_g \ll T_c$. Smallness of the gap distinguishes the system with superconductive islands from usual dirty superconductors. Roughly speaking, it behaves as a continuous 2D superconductor at the energy/temperature scales smaller than E_g, whereas in the range $E_g < (E, T) < T_c$ it can rather be described as an array of weak Josephson junctions.

The existence of the sharp gap (8) in the electron spectrum looks surprising, as only a tiny fraction $(a/b)^2$ of graphene area is in direct contact with SC islands. The presence of this gap can be traced back to the periodic structure of islands we assumed. Therefore any irregularity in the positions of SC islands will lead to the smearing of the hard gap. Assuming that islands' locations are shifted at random from the sites of the ideal triangular lattice, with the typical shift $\delta b \ll b$, one can reduce the problem to the effective one, defined on a scales large than array lattice constant. Random displacements of islands will be seen, in terms of this effective model, as local fluctuations of the superconductive coupling constant [14, 15], leading to the smearing of the gap with the relative width $\delta E_g \sim (\delta b/b)^2 E_g$. The sharp gap will also be smeared by thermal fluctuations of island's phases φ_i and finite thermal coherence length L_T. Thus we expect the spectral gap to be observable at $T \ll E_g$.

Even in the presence of the gap smearing, strong suppression of the local DoS in graphene at $E \le E_g$, should be seen by the low-temperature Scanning Tunnelling Microscopy. The spectral (pseudo) gap is a signature of collective proximity effect which cannot be quantitatively described by a pair-wise interaction between SC islands as soon as low-energy scales $\le E_g$ are involved. The corresponding spatial scale

$$\xi_g = \sqrt{\hbar D/E_g} \sim b\sqrt{\ln(b/a)} \quad (9)$$

plays the role of low-temperature coherence length in the (dirty-limit) superconductor. Under our main condition $\ln(b/a) \gg 1$, the coherence length $\xi_g \gg b$, which allows continuous treatment of the array at low temperatures.

The local superconductive order parameter in graphene, $\mathcal{F}(\mathbf{r}) = \int d\omega\, F_\omega(\mathbf{r})$, can be found at $T < E_g$ as

$$\mathcal{F}(\mathbf{r}) = \sum_j \frac{De^{i\varphi_j}}{(\mathbf{r}-\mathbf{r}_j)^2} \frac{\Theta[t(|\mathbf{r}-\mathbf{r}_j|)]}{\ln(|\mathbf{r}-\mathbf{r}_j|/a)}, \quad (10)$$

where $\mathbf{r}_j$ are the coordinates of SC islands, $t(r) = (G_{\rm int}/2\pi g)\ln(r/a)$, and we used the solution (3) for $\omega > E_g$. The divergent sum in Eq. (10) should be cut at $|\mathbf{r} - \mathbf{r}_j| \sim \xi_g$ since the spectral gap (8) suppresses the lowest-ω contribution to $\mathcal{F}(\mathbf{r})$. Equation (10) is not applicable in the vicinity of SC islands since Eqs. (1) and (2) cannot be linearized at small $|\mathbf{r} - \mathbf{r}_j|$.

At zero magnetic field, φ_j = const and the space-averaged order parameter $\overline{\mathcal{F}}$ is given by

$$\overline{\mathcal{F}} = n_i \int_b^{\xi_g} d^2 r \frac{D}{r^2} \frac{\Theta[t(r)]}{\ln(r/a)} = \frac{\pi^2}{2} n_i D \frac{\ln\ln(b/a)}{\ln(b/a)}, \quad (11)$$

where the last expression refers to the large-$G_{\rm int}$ limit ($\Theta \approx \pi/2$) and $n_i \approx 1/b^2$ is the concentration of SC islands. Comparison of (11) and (8) provides the condition for neglecting the intrinsic Cooper-channel interaction in graphene, λ_g. Namely, its presence would generate the energy gap $\Delta_g = \lambda_g \overline{\mathcal{F}}$. This "intrinsic" gap can be neglected compared to the proximity-induced gap (8) provided that $\lambda_g \ll 0.5$. Comparison with the estimate for intrinsic Cooper interaction constant [7] shows that the latter is indeed negligible.

Electromagnetic response. Linear response of the superconductive film to a weak electromagnetic field is characterized by the superconductive density ρ_s. In the intermediate temperature range, $E_g \ll T \ll T_c$, one can easily calculate ρ_s within the pair-wise approximation for the proximity coupling:

$$\rho_s(T) = \frac{n_i^2}{2} \int_0^\infty 2\pi r^3 E_J(r, T) dr. \quad (12)$$

Taking $E_J(r, T)$ from Eq. (5) we find

$$\rho_s(T) = (\pi^3/3) g A^2 (\pi T) E_{\rm Th}^2/T, \quad (13)$$

where $g = 2\nu_0 D$ and the numerical factor corresponds to the triangular array with $n_i = (2/\sqrt{3})b^{-2}$. At lowest temperatures, $T < E_g$, the function $\rho_s(T)$ saturates at the value that can be estimated by the replacement $T \longrightarrow E_g$ in Eq. (13). For highly transparent interface we obtain

$$\rho_s(0) \approx 10 g E_{\rm Th}/\ln(b/a). \quad (14)$$

Comparing (14) and (8) we find that $\rho_s(0) \approx 4gE_g$, which is typical for dirty superconductors with the gap E_g.

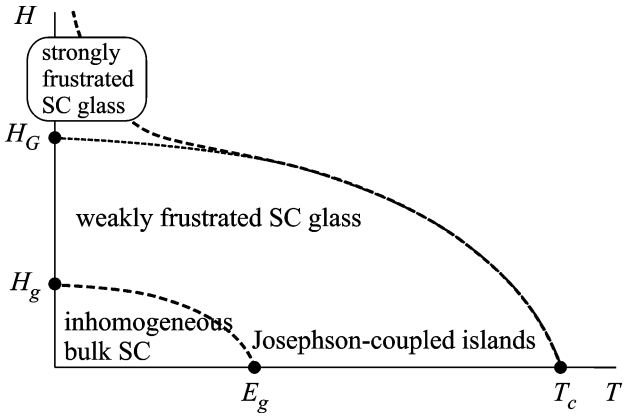

Fig. 3. Schematic phase diagram of the graphene sheet with superconductive islands; all lines refer to crossovers rather than to sharp phase transitions.

The critical current density per unit length at the lowest temperatures, $T \ll E_g$, can be estimated as

$$j_c(0) \approx \frac{2e}{\hbar b} E_J(b,0) = \frac{\pi^3}{2} \frac{egD}{b^3 \ln^2(b/a)}, \qquad (15)$$

where we used, as an estimate, the $T = 0$ limit of the pair-wise Josephson coupling energy (5) at $G_{\rm int}/g \gg 1$:

$$E_J(b,0) = \frac{\pi^3}{4} \frac{gE_{\rm Th}}{\ln^2(b/a)}. \qquad (16)$$

The effect of the transverse magnetic field is characterized by two different field scales:

$$H_g = \frac{\Phi_0}{2\pi\xi_g^2} \approx \frac{0.4}{\ln(b/4a)} \frac{\Phi_0}{b^2}, \quad H_{\rm Glass} = \frac{\Phi_0}{b^2}. \qquad (17)$$

In the low-field, low-T region ($B \ll H_g$ and $T \ll E_g$), magnetic field produces well-separated pancake "hyper-vortices" with the core size $\xi_g \geq b$ (the local DoS is gapless in the core regions). These vortices are strongly pinned by the underlying array structure, so a high critical current $j_{c1} \sim j_c(0)(b/\xi_g)$ is expected. At $B \approx H_g$ vortex cores overlap and the proximity gap is totally destroyed, so H_g is an analogue of the upper critical field H_{c2}. However, the metallic state is not formed right above H_g, at least at $T \ll E_g$. In this field range one deals with a system of frustrated pair-wise Josephson couplings, with full frustration achieved at $B \gg H_{\rm Glass}$. In this high-field range, average values of Josephson coupling are exponentially suppressed, $\overline{E_J(B)} \propto \exp(-B/H_{\rm Glass})$. However, as shown in [16, 17], actual (random-sign) Josephson couplings are much stronger due to mesoscopic fluctuations:

$$E_J^{\rm glass}(b) = [\overline{(E_J(b))^2}]^{1/2} \sim \frac{E_{\rm Th}}{\ln^2(b/a)}, \qquad (18)$$

which is just by the factor $1/g$ smaller than the $(T, B) = 0$ pairwise coupling (16). The estimate (18) shows that at $T \longrightarrow 0$ the superconductive glass state survives up to high magnetic fields $H_{g2}(0) \gg H_{\rm Glass}$. The value of $H_{g2}(0)$ is determined by quantum phase fluctuations [17, 18]:

$$H_{g2} \sim (\Phi_0/b^2) e^{c\sqrt{g}}, \quad c \sim 1. \qquad (19)$$

The overall phase diagram in the (H, T) plane is shown schematically in Fig. 3. We emphasize that the lines indicated do not refer to sharp phase transitions (which are absent in the presence of magnetic field, apart from some special values of frustration for the case of well-defined lattice of islands) but rather mark a crossover regions. Note that determination of T_c for rational values of frustration $f = 1/4, 1/3, 1/2$ (where results for nearest-neighbor XY model are available) is complicated by the necessity of accounting for long-range proximity couplings.

To conclude, we have shown that graphene can be made superconductive with T_c of the order of few Kelvins, due to collective proximity effect induced by small superconductive islands covering only a tiny part of graphene sheet area. The spectral gap is expected at low temperatures $T \ll T_c$ and magnetic fields $B \ll \Phi_0/b^2$. Transformation from a continuous disordered superconductive state to a weakly coupled junction array is predicted with the temperature and/or magnetic field increase.

Our study was based on the standard Usadel equations which are valid for sufficiently disordered samples ($l \ll a$). In the opposite limit of quasi-ballistic electron motion around islands, the Andreev subgap conductance might decrease, leading to the increase of quantum fluctuations of phases $\varphi_i(t)$ [18, 19]. Quantum fluctuations can be neglected under the condition $b^2 \ln(b/a) \ll b_c^2$, where b_c is the critical distance between the islands marking the quantum phase transition (QPT) to the metallic state [18]. The same problem of suppressed Andreev conductance appears to be even more serious with the decrease of the electron density towards the graphene neutral point: scattering cross-section of electrons on the SC islands drops in the range of $k_F a \sim 1$ leading to effective decoupling of island's phases and to strong quantum fluctuations. These fluctuations may lead to the QPT of the superconductor-metal type [18, 19].

We are grateful to P.A. Ioselevich, P.M. Ostrovsky, and M. Titov for useful discussions. This work was partially supported by RFBR grant no. 07-02-00310.

REFERENCES

1. K. Novoselov et al., Science **306**, 666 (2004).
2. A. H. Castro Neto et al., arxiv:0709.1163.

3. H. Heersche et al., Nature **446**, 56 (2007); Xu Du, I. Skachko, and E. Andrei, Phys. Rev. B **77**, 184507 (2008).
4. K. Usadel, Phys. Rev. Lett. **25**, 507 (1970).
5. M. Titov, unpublished.
6. K. S. Tikhonov and S. V. Kopylov, unpublished.
7. In graphene, repulsion in the Cooper channel involves electrons from different valleys (wavevectors near the K and K' points), which means that the Coulomb scattering amplitude is $U_C = 2\pi e^2/(\kappa K_0)$, where $\kappa \approx 5$ is the effective dielectric constant of graphene on the substrate and $K_0 = 1.7 \times 10^8$ cm^{-1} is the distance between K and K' points in the reciprocal space. The dimensionless (repulsive) coupling constant is very small, $-\lambda_g = U_C\nu_0 = (2e^2/\kappa\hbar v_F)(k_F/K_0) \le 0.03$ for $n = k_F^2/\pi < 10^{13}$ cm^{-2}, due to the DOS $\nu_0 = k_F/\pi\hbar v_F$ per single spin projection.
8. M. Yu. Kupriyanov and V. F. Lukichev, Zh. Eksp. Teor. Fiz. **94**, 139 (1987) [Sov. Phys. JETP **67**, 1163 (1988)].
9. B. Huard, N. Stander, J. A. Sulpizio, and D. Goldhaber-Gordon, arXiv:0804.2040.
10. W. Y. Shih and D. Stroud, Phys. Rev. B **32**, 158 (1985).
11. F. V. Tikhonenko, D. W. Horsell, R. V. Gorbachev, and A. K. Savchenko, Phys. Rev. Lett. **100**, 056802 (2008).
12. A. A. Golubov and M. Yu. Kupriyanov, Sov. Phys. JETP **69**, 805 (1989).
13. P. M. Ostrovsky, M. A. Skvortsov, and M. V. Feigel'man, Phys. Rev. Lett. **87**, 027002 (2001).
14. A. I. Larkin and Yu. N. Ovchinnikov, Zh. Eksp. Teor. Fiz. **61**, 2147 (1971) [Sov. Phys. JETP **34**, 1144 (1972)].
15. J. S. Meyer and B. D. Simons, Phys. Rev. B **64**, 134516 (2001).
16. B. Spivak and F. Zhou, Phys. Rev. Lett. **74**, 2800 (1995).
17. V. M. Galitskii and A. I. Larkin, Phys. Rev. Lett. **87**, 087001 (2001).
18. M. V. Feigel'man, A. I. Larkin, and M. A. Skvortsov, Phys. Rev. Lett. **86**, 1869 (2001).
19. M. V. Feigel'man and A. I. Larkin, Chem. Phys. **235**, 107 (1998).